Design and Control of a Single Phase DC/Rectified AC/AC Inverter for low THD Applications

Burak Tekgun* Didem Tekgun*
*Department of Electrical Electronics Engineering,
Abdullah Gul University,
Kayseri/Turkey

Irfan Alan* Mohamed Badawy**
**Department of Electrical Engineering
San Jose State University
San Jose, CA, USA

***Abstract*— In this paper, a single phase DC/Rectified AC/AC (DC/RAC/AC) inverter is analyzed and compared to classical single phase PWM inverters. A traditional AC power supply (PS) system consists of a DC/DC converter, a cascaded H-bridge inverter, and a passive filter to generate the sinusoidal output voltage. The presented DC/RAC/AC inverter has a similar structure; however, the control of the cascaded units differ. The presented method generates rectified sine wave at the output of the DC/DC converter unit and the H-bridge inverter alternates the rectified sine wave to generate the full sine wave without having an additional output filter; hence, the switching losses at the H-bridge inverter is limited to the line frequency (50-60 Hz). Moreover, the bulk DC bus capacity at the output of the DC/DC converter is reduced significantly. Therefore, the power consumed by the passive elements are minimized. The circuit modes of operation are analyzed and the system is simulated in Matlab/Simulink environment for both traditional and proposed topologies. Results show that the proposed system is superior to the traditional one in terms of efficiency, generated THD with a simplified control structure, and it offers a reduced system size and cost.**

Keywords—inverter; high efficiency; low THD; low cost; reduced size; sine wave generation; wide band gap; fast control

I. INTRODUCTION

Today, DC to AC power conversion systems are widely used in many applications with different sizes from a few hundred Watts to several hundred kWs or even MW levels. Along with the applications that require uninterruptible power supply, they are used in the systems that use the energy from the batteries or other energy storage systems such as the renewable energy systems that have irregular power flows due to the varying conditions of the source. Since the energy efficiency is one of the major concerns worldwide, the efficiency of such systems is of critical importance.

Typically, a single phase AC PS consists of a DC/DC converter to step up or down the battery voltage and a half bridge or an H-bridge inverter and a passive filter to generate the sine wave on the output as shown in Fig.1.a.

Each of these units has a different control structure where the DC/DC converter may be controlled by a simple proportional-integral voltage or current controller, the H-bridge inverter needs to be controlled with a special control algorithm to generate a low THD sine wave voltage at the output, that should be robust to the disturbances due to the nonlinear loads and has a fast dynamic response to the rapid load variations [1]. During this operation, a high-frequency switching occurs both in the DC/DC converter unit and the H-bridge inverter which causes high switching losses on both units. The proposed single phase PS unit employs a bi-directional DC/DC converter for generating a rectified sine wave on its output and H-bridge inverter switches twice in one period to alternate the rectified sine wave as illustrated in Fig 1.b. Therefore, the switching losses only occur in DC/DC converter unit of the PS as the losses in the H-bridge inverter is negligible. In addition to that, the passive output filter is eliminated and the bulk DC bus capacitor is reduced significantly which result in reduced losses associated with the passive components. Moreover, the losses will further be decreased with the wide bandgap devices used in the system as the remaining passive components and their parasitics get even smaller, which also leads to an increase in the power density of the inverter.

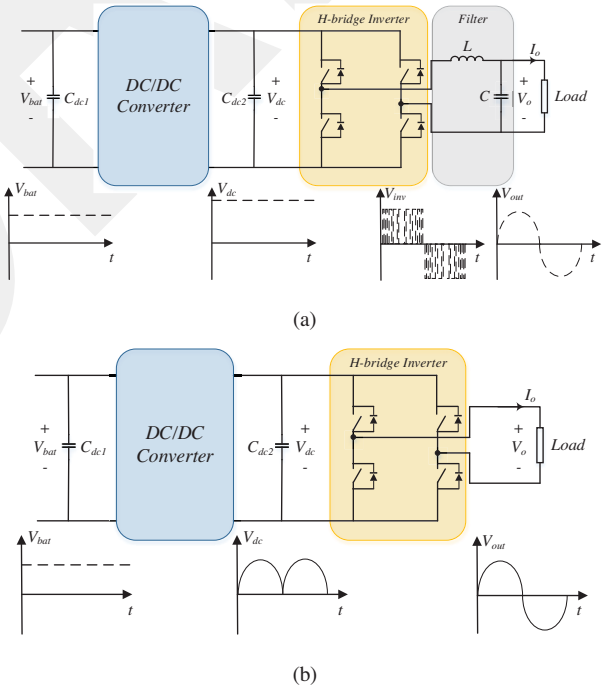

Figure 1. (a) Traditional and (b) proposed single phase PS topology and corresponding signal waveforms.

Buck-boost DC/AC inverters started to attract the attention of the researchers in early 2000s [2] to be used in applications

978-1-5386-5982-3/18/$31.00 ©2018 IEEE

where an overlapping output voltage is needed using a low-cost solution. Additionally, a fast dynamic response might be required, especially in photovoltaic (PV) and fuel cell energy systems [3], [4]. A half bridge series resonant buck-boost inverter is reported in [2]. Although this system is able to generate the sine wave even with low DC bus voltage levels, THD of the generated voltage is quite high. Flyback topology is also used in many applications [5]–[7]. The flyback converter operating in discontinuous conduction mode (DCM) is used excessively in PV applications due to its low cost and simplicity [7]. In order to improve the efficiency, flyback converters are operated in continuous conduction mode (CCM) [6] while reducing the freewheeling current [5]. However, its transfer function contains a right half plane zero that makes the control rather challenging [6]. Various modifications of buck-boost converter topologies can be found in literature. One of the featured versions is reported in [8] where the sine wave is generated with a buck-boost converter cascaded with an unfolding H-bridge inverter. The capacitor current is used to control the converter duty cycle. Although this method is simple and straightforward, the light load performance is not satisfactory and the THD of the output signal is not low because the converter is not operating in a bidirectional mode to discharge the output capacitor for being able to control the negative rate of change of the voltage. In [9], a similar approximation is made but with a passive resonant circuit for soft switching operation. The system has high efficiency at rated loading conditions but there are voltage spikes at the zero crossing instants which affect the THD significantly. Also, this topology cannot operate when the power factor (PF) is not unity as it cannot process the reactive power flow bidirectionally. Bidirectional topologies are more favored for grid-connected renewable energy inverters [10]–[12] as they need to operate in both ways to generate/absorb reactive power while maintaining high-efficiency levels. Additionally, bidirectional topologies are used in fuel cell applications as backup sources to compensate for the effects caused by slow system dynamics [4], [13]. Z source inverters are also considered for grid-connected systems [14]. In addition to these applications, mentioned buck-boost DC/Rectified AC/AC (DC/RAC/AC) inverters are even used for scalar motor control applications as in [15].

In this work, a bidirectional buck-boost inverter is used for single phase PS applications. The inverter is controlled with a modified PI controller. Low THD levels and high efficiency is targeted over a wide range of loading conditions. The following section gives the details of the proposed circuit and the control system. Performance analysis through Matlab / Simulink simulations is given in Section III. Section IV concludes the study and discusses the future improvements.

II. DC / Rectified AC / AC Inverter Topology

A. Circuit Topology

The proposed inverter consists of a bidirectional buck-boost converter and a full bridge inverter as shown in Fig. 3. The buck-boost stage has two fast switches with antiparallel diodes, an inductor, and an output capacitor, and the unfolding circuit has four low-frequency switching switches with antiparallel diodes. The output capacitor of the DC/DC converter is placed after the unfolding circuit to filter out the full bridge inverter switching noise which may occur due to the switching dead time.

Selection of the fast switching devices needs to be done carefully as the primary concern is to improve the efficiency. The switches on the unfolding circuit can be selected as low-cost IGBTs as they do not need to switch at high frequency.

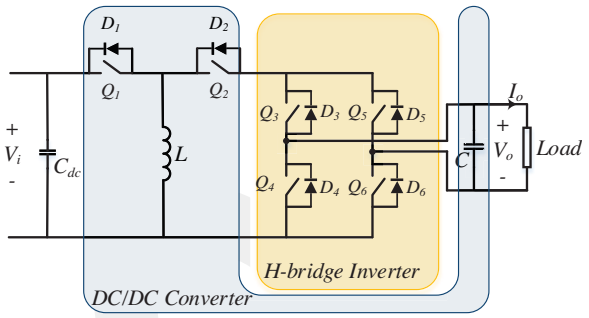

Figure 3. Proposed single-phase DC/DC inverter topology.

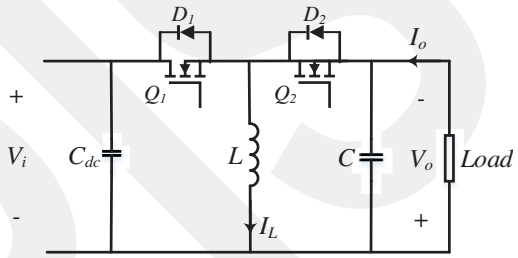

Figure 4. Bidirectional buck-boost converter.

B. Circuit Analysis

The circuit can be analyzed as a well-known buck-boost converter shown in Fig. 4, where, V_i is the input voltage C_{dc} is the DC side capacitor, L and C are the filter inductor and capacitor, D_1, D_2 are the reverse diodes, Q_1 and Q_2 are the switching elements, V_o and I_o are the output voltage and the current, and I_L is the inductor current. In this application, the DC/DC converter is operated in a different way than it is operated usually. Since the output of the buck-boost converter is a rectified sine wave, the output current also follows a similar pattern and it may have a phase angle depending on the load. Therefore, the system should be able to operate even if the PF is not unity. In case the PF is not unity, there will be reactive power circulating through the converter. This means that the converter should be able to operate bidirectionally.

In order to operate the converter bidirectionally and switch between producing and regenerating modes rapidly, the inductor current needs to be discontinuous as the rate of change of output voltage depends on the inductor current direction. When the inductor current is positive, it charges the output capacitor, and if negative, it discharges the output capacitor. This allows us to control the negative rate of change of voltage; hence, a fast dynamic response for the control of rectified sine wave can be achieved. Therefore, for this particular application, the convertor`s operation mode is selected as discontinuous conduction mode (DCM) and the power stage is designed to

keep the converter operating in DCM for a wide range of loading conditions.

In Fig. 5.a and b, the active circuit components can be seen when the power is flowing to and from the converter output. When the converter is providing power to the output, Q_1 and D_2 switches are operating; and when the converter is drawing power from the output, Q_2 and D_1 switches are operating.

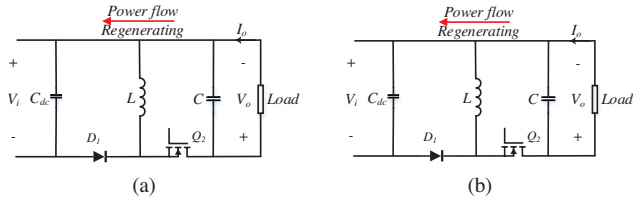

Figure 5. (a) Forward and (b) backward power flow modes.

Constant and varying load conditions can be analyzed by looking at the output voltage and current waveforms when the PF is varying. For a 50 Hz AC system, Fig. 6.a. and 6.b show the output voltage and current waveforms when the PF is unity with producing (Fig. 6.a) and regenerating (Fig. 6.b) conditions. Fig. 7 shows the output current and voltage waveforms along with the instantaneous power waveform for non-unity PF operation.

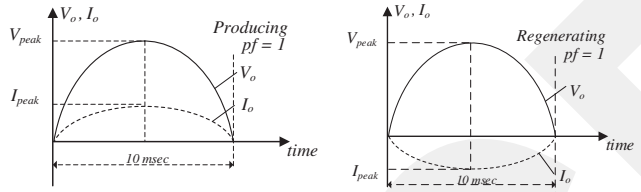

Figure 6. DC/DC converter output voltage and current when (a) the power is produced and when (b) the power regenerated with unity PF.

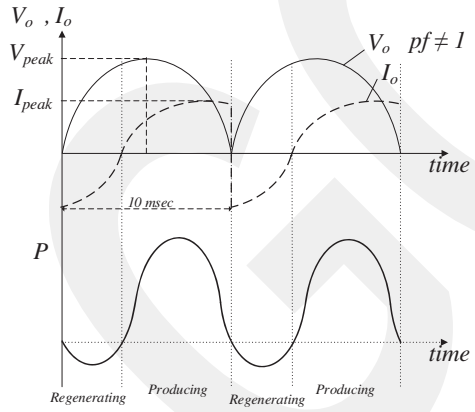

Figure 7. DC/DC converter output voltage, current and instantaneous power with non-unity power factor.

In this type of operation, the output voltage and the load are constantly varying, thus, the power stage design becomes a challenge as the DCM is desired for a wide range of operation. Hence, the inductor and capacitor values should be determined for the rated condition with unity PF, then these values should be verified for the non-unity PF operation.

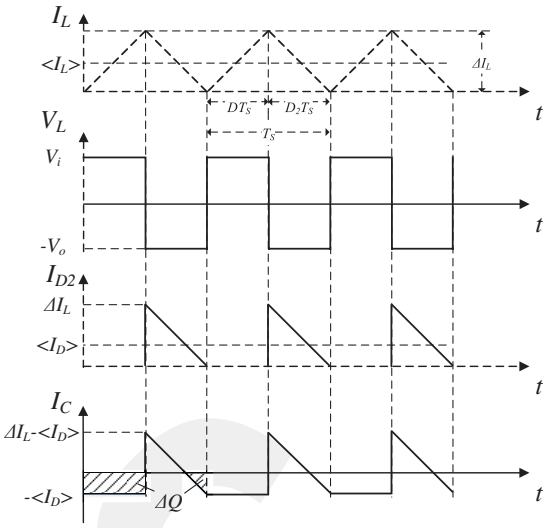

Figure 8. Buck-boost converter waveforms at the CCM-DCM boundary

The maximum inductance value for maintaining DCM can be determined by the following procedure. First, the maximum output current is determined as critical current. If the system is operating at the boundary of DCM and CCM (Continuous conduction mode), the inductor current and voltage will look like in Fig. 8. The critical output current, $I_{o(crit)}$, is basically half of the peak inductor current, ΔI_L. Second, the inductance value is calculated using the inductance voltage and current relations as follows:

$$\Delta I_{L(+)} = \frac{V_i}{L} DT_S = \Delta I_{L(-)} = \frac{V_o}{L} D_2 T_S \quad (1)$$

$$L_{\max} \le \frac{V_o T_S V_i}{2 I_{o(crit)} \left(V_o - V_i\right)} \quad (2)$$

where, T_S is the switching period, D is the duty cycle, D_2 is the off state duty cycle.

After determining the inductance value, the output capacitor value can be determined based on the capacitor charge variation, i.e. calculating the area of the capacitor current on either positive or negative side and equating that area to the desired voltage ripple as follows:

$$\Delta Q = C \Delta V \quad (3)$$

As it is mentioned above, the system is desired to be operated in DCM at all times but it is not possible to achieve that because PF variation limits the DCM operation range. To illustrate the effect of decreasing power factor, Fig. 9 shows the voltage and current waveforms with different PF values. When the system is operating at point A, the output voltage is at its max value and the current is less than its rated peak value, which guarantees that the system operates in DCM because the inductance value is determined for the peak output current, current levels less than this value result in DCM operation. For the same PF value, if the output voltage gets close to zero (point B), the current does not fall down to zero and keeps flowing. This condition is where the challenge starts because this current forces to the system to

operate in CCM. The worst case scenario occurs when the PF is zero (point C); current is at its max value and the voltage is zero. Hence, while designing the power stage, it is crucial to maximize the use of DCM while keeping the reasonable inductor current ripple as it is the source of current stress on the switching devices.

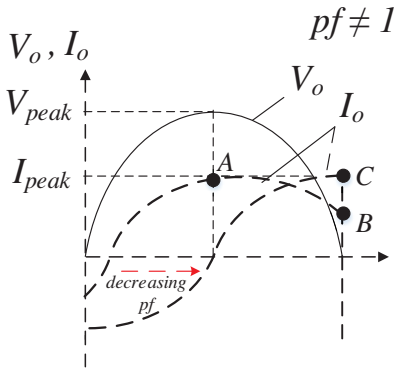

Figure 9. Variation of the operating condition as the power factor is decreasing.

A similar approach can be followed for the regenerating condition. This time the output voltage becomes the input voltage and the DC input voltage becomes the output voltage for the converter.

It should be kept in mind that if the converter is desired to be operated in DCM at all times, either an additional inductor parallel to the first one can be switched on and off or the inductor current ripple can be selected quite high, which makes the inductor small. The first solution puts additional cost and control effort, and the latter one increases the current stress which is not desirable as it affects the cost, the reliability and the lifetime of the converter. In this work, the inductor value is selected to operate for the PF to be in between 0.5 and 1 range for both power directions.

C. System Control

A PI controller controls both the forward and backward power flows by switching between its modes of operation based on the error signal. The reference and the measured inverter output voltage are rectified to operate in positive DC region. The error is fed to the PI controller. If the error is positive the power flows from the DC input to the circuit output and only gate 1 is active (Q_1 and D_2 are alternating). When the error is negative the power is flowing from the circuit output to the DC input and only gate 2 is active (Q_2 and D_1 are alternating). Therefore, the calculated duty ratio for the forward operation needs to be reversed for the backward operation considering that the output voltage becomes the input voltage and DC input voltage becomes the output as illustrated in Fig. 10.

The RAC/AC conversion block, the H bridge inverter, is controlled based on the electrical angle, theta (θ), generated for the reference sine wave. For the grid-tied inverters, this angle is determined through a phase locked loop (PLL) algorithm [16]. The controller turns on the switches Q_3 and Q_6 when θ is smaller than π, and Q_4 and Q_5 when theta is greater than π to alternate, i.e. unfold, the generated rectified sine wave.

This simple and straightforward control allows the system to operate in bidirectional manner. Thus, the system operates effectively even at non-unity PF values.

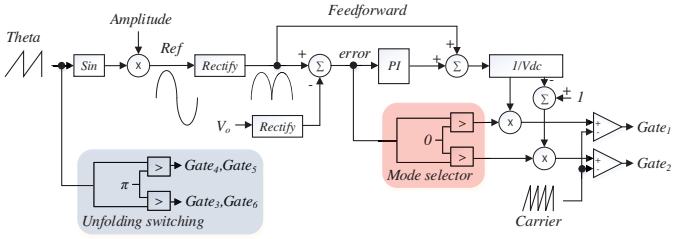

Figure 10. Proposed control strategy.

III. Performance Analysis

In order to evaluate the proposed systems efficacy, a simulation study is done in MATLAB/Simulink environment. Using the same conditions, traditional and proposed systems are simulated while switching losses and efficiencies are compared for various loading and PF conditions. The THD is analyzed under various load current waveforms.

The output voltage of the system is 220 Vrms, 50 Hz, the input voltage is 250 Vdc, and the converter power is 250 VA. SiC MOSFETs are selected for this application to benefit the high-frequency switching and consequently reduce the sizes and losses of the passive elements. The switching frequency is selected as 150 kHz as this value is the limit for safe and efficient operation determined by the SiC MOSFET manufacturers. The inductor current ripple is selected as 10 A, and the output voltage ripple is selected as 0.5% of the max voltage, which is roughly 1.5 V. Based on these specifications and using equations (1), (2), and (3), maximum inductor value is calculated as 92 µH, and minimum capacitor value is calculated as 9.92 µF. Hence, the inductor and capacitor values are selected as 90 µH, and 10 µF. The inductor value can be selected even smaller; however, this would increase the peak inductor current, which causes higher current stress on the switches and lower THD as the pulsating current charging the output capacitor increase. Considering the peak output current is 1.614A, the system maintains DCM between 0.5 and 1 PF when the output voltage is higher than 20 V.

To compare the proposed and conventional topology only in terms of efficiency and THD, all the active switches are selected as SiC MOSFETs. The ON resistance of the switch is 65 mΩ, output capacitance is 60 pF, parasitic inductance is 10 nH per switch, and the diode forward voltage drop is 4.4 V. To make a fair comparison between the topologies, the conventional system is also operated at the same frequency (150 kHz), the DC/DC converter filter values are selected as 110 µH, and 25 µF, H bridge inverter's output LC filter is selected as 150 µH, and 10 µF for 40 kHz cutoff frequency, which also has equivalent series resistances 15 mΩ and 5 mΩ, respectively. The cutoff frequency is selected to achieve pest possible THD.

A. Efficiency Analysis

In order to emphasize the superiority of the proposed topology over the conventional one presented in Fig. 1.a, the converter is simulated at the rated loading condition with unity

PF first. Total switching loss is calculated as 6.9 W, measured THD is 0.41%. The same condition is simulated with the traditional inverter with a worse THD (77%) without LC filter at the output and with a similar THD (0.43%) with LC filter at the output and the switching loss is calculated as 10.5 W. The switching loss is reduced around 34%. In the traditional topology, in addition to the switching losses which occur in both DC/DC and unfolding stages, there are two more passive elements to filter out the output voltage that cause the loss to increase even more. Calculated efficiency for proposed and traditional topologies are 94.3% and 92.1%, respectively.

Later, the proposed and conventional converter topologies are simulated with 25% to 100% of rated load and 0.5 to 1 PF variation to compare the efficiencies and THDs. Fig 11.a, b, c, d, and e show the comparison of the efficiencies for PFs of 0.5, 0.7, 0.8, 0.9, and 1.

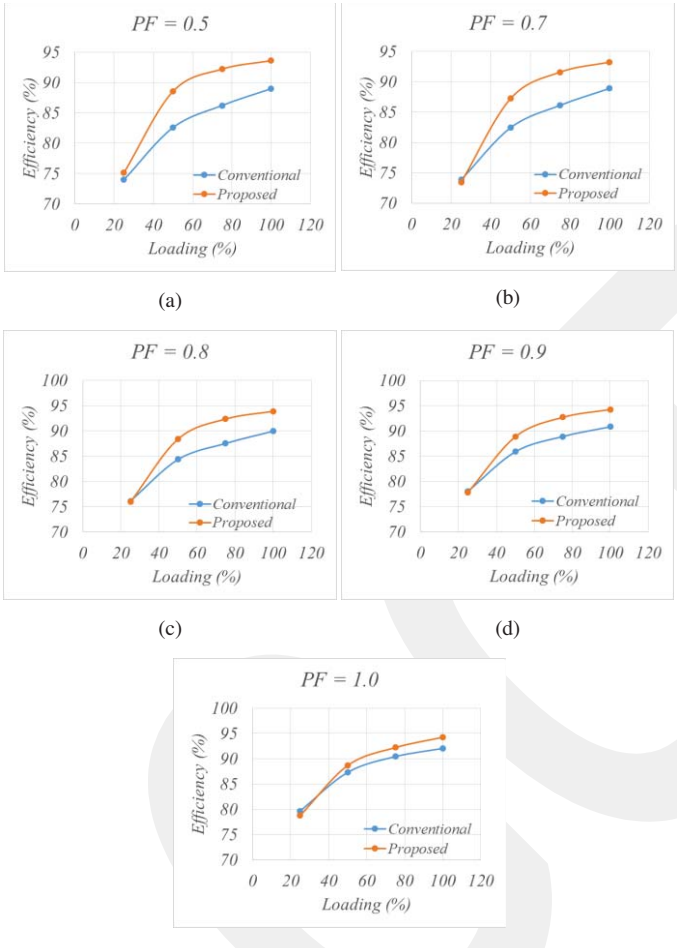

Figure 11. Comparison of the efficiencies of proposed and conventional converter topologies simulated with 25% to 100% of rated loading with (a) 0.5, (b) 0.7, (c) 0.8, (d), 0.9, and (e) 1 power factors.

It can be clearly seen that the efficiency of the proposed converter is superior to the conventional at different operating conditions.

B. THD Analysis

The THD analysis for the varying PF and loading conditions are done as presented in Fig. 12. It should be noted that the conventional converter control is done separately for the DC/DC converter and DC/AC inverter. Voltage control scheme is used in the DC/DC converter with a PI feedback controller, and simple PI voltage tracking is used to control the H bridge inverter rather than a complex control scheme. Therefore, the comparison is not done for nonlinear loading conditions as the conventional system is not able to regulate the voltage properly for nonlinear loading in its current form.

Fig 12.a, b, c, d, and e show the comparison of the THDs for PFs of 0.5, 0.7, 0.8, 0.9, and 1. Clearly, the proposed system has lower THD values at all the load conditions.

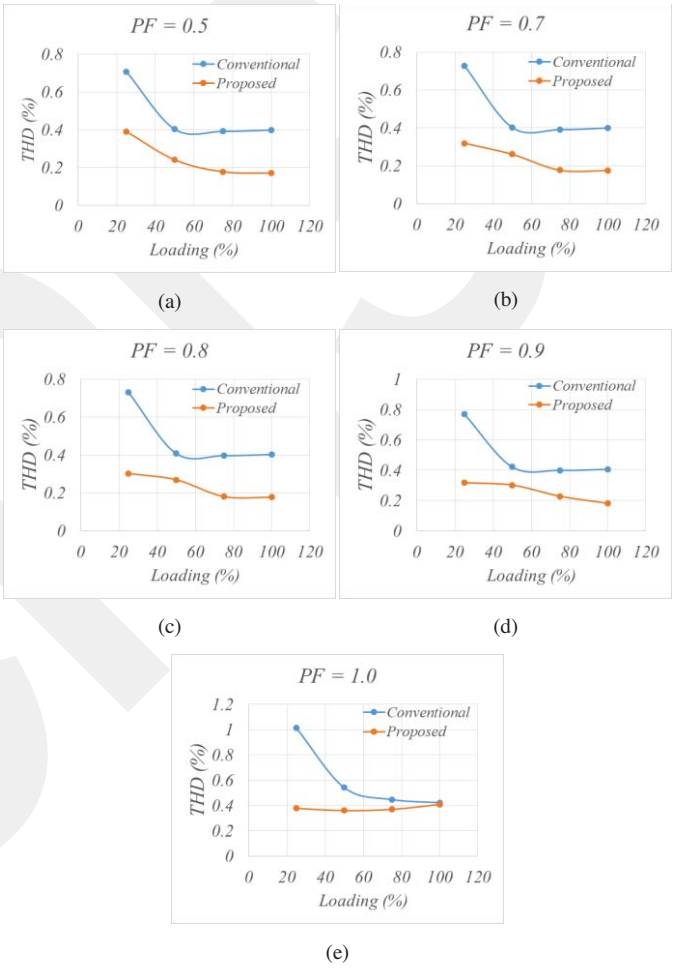

Figure 12. Comparison of the THDs of proposed and conventional converter topologies simulated with 25% to 100% of rated loading with (a) 0.5, (b) 0.7, (c) 0.8, (d), 0.9, and (e) 1 power factors.

The single-phase classical inverter control under nonlinear loading conditions has been a challenge and many respective works can be found in the literature [1], [8], [17], [18]. Repetitive control, deadbeat control, Lyapunov function based control are some of these control methods which require quite complex calculations for the design. The proposed system has a fast dynamic response such that it has 0.22% THD under square wave current waveform as shown in Fig. 13.a. THD increases to

1.1% for the waveforms that have a crest factor of 3 as given in Fig.13.b and c, where power flow directions are in opposite directions and the system is operating at 135% load.

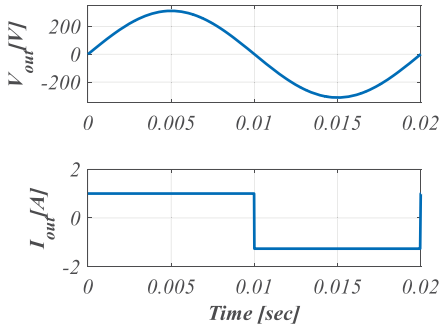

(a)

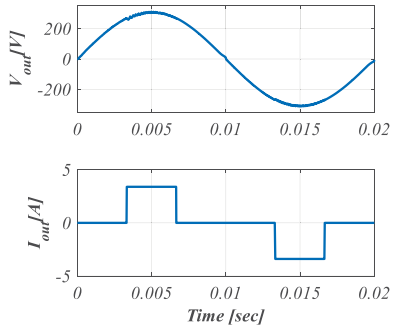

(b)

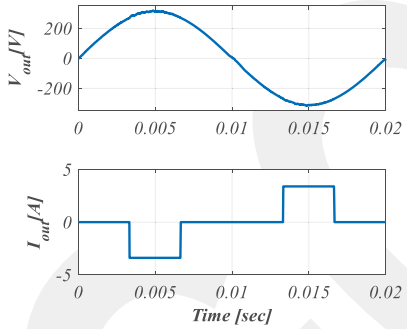

(c)

Figure 13. Output voltage waveforms under various nonlinear loads. (Current waveforms are (a) square wave, (b) pulse that has a crest factor of 3 and same pulse in opposite direction.)

IV. Conclusions

In this study, a DC/RAC/AC inverter topology is presented along with its control structure. A bidirectional buck-boost converter is used to generate rectified sine waves and a full bridge unfolding circuit switches at twice of the line frequency to generate a full sine wave voltage at the output side. This simple approximation makes the sinusoidal voltage generation simpler than conventional approaches as it eliminates the output passive filter and reduces the size of the DC bus capacitor. Thus, the proposed system has lower cost, reduced size and higher efficiency due to the reduction in the switching losses. Additionally, the control structure is simplified and the THD levels are lowered. Highest observed THD for various nonlinear loading conditions is 1.1%, which is much lower than the required max THD level standardized by IEEE for low voltage applications (5%) [19]. The theory of operation of the circuit and the control algorithm are explained, simulations are performed at various loading conditions to verify the efficacy of the proposed system. Simulation results show that the switching losses are 34% lower than the traditional sinusoidal voltage generating systems for rated conditions.

References

[1] B. Tekgun, A. R. B. Chowdhury, M. A. Mahmood, and Y. Sozer, "Design and implementation of a sinusoidal flux controller for core loss measurements," in *2016 IEEE App. Pow. Electron. Conf. and Expo. (APEC)*, 2016, vol. 2016–May, pp. 207–214.

[2] Chien-Ming Wang and Teng-Jen Chen, "Novel single-stage half-bridge series-resonant buck-boost inverter," *IEEE Trans. Aerosp. Electron. Syst.*, vol. 40, no. 4, pp. 1262–1270, Oct. 2004.

[3] D. Voglitsis, N. Papanikolaou, and A. C. Kyritsis, "Incorporation of Harmonic Injection in an Interleaved Flyback Inverter for the Implementation of an Active Anti-Islanding Technique," *IEEE Trans. Power Electron.*, vol. 32, no. 11, pp. 8526–8543, 2017.

[4] A. R. Boynuegri, "A power management unit with a polarity changing inverter for fuel cell/ultra-capacitor hybrid power systems," *Int. J. Hydrogen Energy*, vol. 42, no. 43, pp. 26924–26932, 2017.

[5] Fanghua Zhang and Chunying Gong, "A New Control Strategy of Single-Stage Flyback Inverter," *IEEE Trans. Ind. Electron.*, vol. 56, no. 8, pp. 3169–3173, Aug. 2009.

[6] H. Kim, J. S. Lee, and M. Kim, "Downsampled Iterative Learning Controller for Flyback CCM Inverter," *IEEE Trans. Ind. Electron.*, vol. 65, no. 1, pp. 510–520, Jan. 2018.

[7] Y. Li and R. Oruganti, "A low cost flyback CCM inverter for AC module application," *IEEE Trans. Power Electron.*, vol. 27, no. 3, pp. 1295–1303, 2012.

[8] M. Çelebi and I. Alan, "A novel approach for a sinusoidal output inverter," *Electr. Eng.*, vol. 92, no. 7–8, pp. 239–244, 2010.

[9] J. Madouh, N. A. Ahmed, and A. M. Al-Kandari, "Advanced power conditioner using sinewave modulated buck-boost converter cascaded polarity changing inverter," *Int. J. Electr. Power Energy Syst.*, vol. 43, no. 1, pp. 280–289, 2012.

[10] A. A. Khan, H. Cha, H. F. Ahmed, J. Kim, and J. Cho, "A Highly Reliable and High-Efficiency Quasi Single-Stage Buck-Boost Inverter," *IEEE Trans. Power Electron.*, vol. 32, no. 6, pp. 4185–4198, 2017.

[11] W. Wu, J. Ji, and F. Blaabjerg, "Aalborg Inverter - A New Type of 'Buck in Buck, Boost in Boost' Grid-Tied Inverter," *IEEE Trans. Power Electron.*, vol. 30, no. 9, pp. 4784–4793, Sep. 2015.

[12] Y. Tang, X. Dong, and Y. He, "Active Buck–Boost Inverter," *IEEE Trans. Ind. Electron.*, vol. 61, no. 9, pp. 4691–4697, Sep. 2014.

[13] M. Jang, M. Ciobotaru, and V. G. Agelidis, "A single-stage fuel cell energy system based on a buck-boost inverter with a backup energy storage unit," *IEEE Trans. Power Electron.*, vol. 27, no. 6, pp. 2825–2834, 2012.

[14] O. Husev, R. Strzelecki, F. Blaabjerg, V. Chopyk, and D. Vinnikov, "Novel Family of Single-Phase Modified Impedance-Source Buck-Boost Multilevel Inverters With Reduced Switch Count," *IEEE Trans. Power Electron.*, vol. 31, no. 11, pp. 7580–7591, Nov. 2016.

[15] F. Karbakhsh, M. Amiri, and H. Abootorabi Zarchi, "Two-switch flyback inverter employing a current sensorless MPPT and scalar control for low cost solar powered pumps," *IET Renew. Power Gener.*, vol. 11, no. 5, pp. 669–677, 2017.

[16] A. Elrayyah, Y. Sozer, and M. Elbuluk, "Robust phase locked-loop algorithm for single-phase utility-interactive inverters," *IET Power Electron.*, vol. 7, no. 5, pp. 1064–1072, May 2014.

[17] H. Komurcugil, N. Altin, S. Ozdemir, and I. Sefa, "An extended

lyapunov-function-based control strategy for single-phase UPS inverters," *IEEE Trans. Power Electron.*, vol. 30, no. 7, pp. 3976–3983, 2015.

[18] S. Kim, S.-H. Lee, J. S. Lee, and M. Kim, "Dual-mode flyback inverters in grid-connected photovoltaic systems," *IET Renew. Power Gener.*, vol. 10, no. 9, pp. 1402–1412, Oct. 2016.

[19] IEEE, *IEEE Recommended Practices and Requirements for Harmonic Control in Electrical Power Systems IEEE Recommended Practices and*, vol. 1992, no. June. 1992.